Dynamic Fracture Toughness Determined from Load-point Displacement

by C. Bacon, J. Färm and J.L. Lataillade

ABSTRACT—The paper presents a method to determine dynamic fracture toughness using a notched three-point bend specimen. With dynamic loading of a specimen there is a complex relation between the stress-intensity factor and the force applied to the specimen. This is due to effects of inertia, which have to be accounted for to evaluate a correct value of the stress-intensity factor. However, the stress-intensity factor is proportional to the load-point displacement if the fundamental mode of vibration is predominant in the specimen. The proportionality constant depends only on the geometry and stiffness of the specimen. In the present method we have measured the applied force and load-point displacement by a modified Hopkinson pressure bar, where two-point strain measurement has been used to evaluate force and displacement for times greater than the transit time for elastic waves in the Hopkinson bar. We have compared the method with the stress-intensity factor derived from strain measurement near the notch tip and good agreement was obtained. The method is well suited for high-temperature testing and results from fracture toughness tests of brittle materials at ambient and elevated temperatures are presented.

Introduction

Three-point bend specimens are widely used for determination of static fracture toughness, K_{Ic}, as well as dynamic fracture toughness, K_{Id}. To evaluate the fracture toughness two quantities must be known, namely, the stress-intensity factor, $K_I(t)$, and the time, t_i, for initiation of crack growth. Under static conditions, the stress-intensity factor, K_I, is proportional to the applied force. Under impact loading, this proportionality does not hold due to effects of inertia.[1,2] If the time to fracture is sufficiently long, however, quasi-static conditions at the time for initiation of crack growth can be assumed and therefore the static formula can be used. Server has presented a procedure for performing such a quasi-static test.[3]

Many authors have studied the problem to evaluate the dynamic stress-intensity factor, $K_I(t)$, and several techniques have been proposed. One possibility is to calculate the stress-intensity factor from a local measurement made near the crack tip and thereby avoiding problems with effects of inertia. Most common are strain-gage measurements or optical techniques such as the caustic method and methods based on photoelasticity.[4] Other techniques make use of modeled dynamic behavior of the specimen to account for effects of inertia. The model can be a finite-element model or an approximative analytical one.[5,6]

Kishimoto *et al.*[5] assumed a linear relation between the dynamic stress-intensity factor and the load-point displacement. A two-dimensional finite-element analysis confirmed that assumption. They calculated the load-point displacement from the applied force using the relation obtained by Nash.[7]

The standard techniques for impact loading have been the instrumented Charpy test and the drop-weight test. The applied force has been measured by strain gages on the Charpy striker or on a striker tup but the impact velocity has remained undetermined.

The Hopkinson pressure bar technique[8] makes it possible to measure both the applied force and the load-point velocity. Integration of the velocity gives the load-point displacement. The conventional Hopkinson bar method does not allow calculation of the applied force and load-point displacement when the time to fracture is longer than the transit time of the elastic waves in the bar.

The method presented in this paper is based on the assumption of a linear relation between the stress-intensity factor and the load-point displacement measured by a modified Hopkinson pressure bar. Two-point strain measurement[9] has been used to evaluate

C. Bacon is Assistant Professor, Laboratoire de Mécanique Physique, Université de Bordeaux I, 351 Cours de la Libération, 33 405 Talence Cedex, France. J. Färm is Assistant Professor, Swedish Institüte for Materials Technology, IMT, Sundsvall, S-851 71 Sundsvall, Sweden. J.L. Lataillade is Professor in Mechanics, Ecole Nationale Supérieure des Arts et Métiers, Esplanade des Arts et Métiers, 33 405 Talence Cedex, France.

Original manuscript submitted: October 5, 1992. Final manuscript received: October 15, 1993.

the applied force and the load-point velocity. This method extends the time interval that can be studied. We have compared our method with a more direct one, where the stress-intensity factor was derived from strain measurements near the notch tip on a three-point bend specimen. There was a good agreement between the two methods. A specific advantage with our method is that high-temperature tests are easy to perform. Fracture toughness tests have been made on brittle materials at both ambient and elevated temperatures.

Evaluation of Dynamic Fracture Toughness

The dynamic fracture toughness, K_{Id}, is a material property, which depends on both the temperature and the rate of loading. It is equal to the value of the dynamic stress-intensity factor, $K_I(t)$, at the time, t_i, of initiation of crack growth.

$$K_{Id} = K_I(t_i) \tag{1}$$

Thus, to determine the dynamic fracture toughness the stress-intensity factor at the time of initiation of crack growth must be known. Since the time derivative, $\dot{K}_I(t)$, is normally used to represent the rate of loading, the full time history, $K_I(t)$, and the time, t_i, are needed from dynamic tests. Moreover, the rate of loading should be kept constant during the test. Three-point bend specimens have a nearly constant $K_I(t)$ during dynamic loading. We have used such specimens for the evaluation of the fracture toughness.

Dynamic Stress-intensity Factor

The dynamic stress-intensity factor, $K_I(t)$, is[10]

$$K_I(t) = \lim_{r \to 0} [\sqrt{2\pi r}\, \sigma_{22}(r, \theta = 0, t)] \tag{2}$$

where σ_{22} is the stress perpendicular to the crack direction. In bending of crack-free beams this stress is proportional to the bending moment, and it is supposed that this relation holds also when a crack is present. Thus, the bending moment at the midspan of the specimen will be proportional to the dynamic stress-intensity factor.

Nash has made an analysis of the forces and bending moments in a notched three-point bend specimen[6] where he considered all symmetric modes of vibration. If the first mode is assumed to be predominant in the specimen it follows from his analysis that the load-point displacement is proportional to the bending moment and thereby also to the stress-intensity factor. Kishimoto *et al.*[5] have assumed and verified proportionality between load-point displacement and stress-intensity factor through comparison with two-dimensional finite-element solutions for step loading and for final-peak-sawtooth-pulse loading.

The dynamic stress-intensity factor can, with the assumption of first mode vibration only, be expressed as

$$K_I(t) = Cu(t) \tag{3}$$

where u is the load-point displacement and C is a constant. This expression is valid also under static conditions.

The static stress-intensity factor, K_I, is expressed by Tada *et al.*[11] for the specimen geometry in Fig. 1 as

$$K_I = \frac{3S\sqrt{a}}{2BW^2} Y\left(\frac{a}{W}\right) F \tag{4}$$

where F is the applied force and Y is a calibration function. According to Srawley[12] this function is given for specimens with $S/W = 4$ by

$$Y\left(\frac{a}{W}\right) = \frac{1.99 - \frac{a}{W}\left(1 - \frac{a}{W}\right)\left(2.15 - 3.93\frac{a}{W} + 2.7\left(\frac{a}{W}\right)^2\right)}{\left(1 - 2\frac{a}{W}\right)\left(1 - \frac{a}{W}\right)^{3/2}} \tag{5}$$

Equations (3) and (4), together with the static relation $F = k$u, give

$$C = \frac{3S\sqrt{a}}{2BW^2} Y\left(\frac{a}{W}\right) k \tag{6}$$

where k is the specimen stiffness. With eq (6) inserted into eq (3) the dynamic stress-intensity factor can be written as

$$K_I(t) = \frac{3S\sqrt{a}}{2BW^2} Y\left(\frac{a}{W}\right) ku(t) \tag{7}$$

Evaluation of Load-point Displacement and Applied Force

The normal force and particle velocity at the end of the modified Hopkinson pressure bar shown in Fig. 2 were obtained from the measured strains $\varepsilon_A(t)$ and

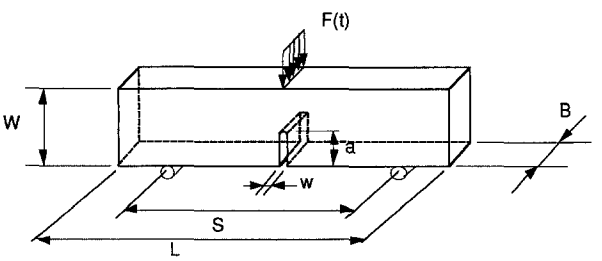

Fig. 1—Three-point bend specimen

$\varepsilon_B(t)$ at x_A and x_B, by use of the method developed by Lundberg *et al.*[9] This method applies to nonuniform rods, and we have used the special case of a uniform rod with Young's modulus E, density p, and cross-section area A. The wave propagation speed is $c = \sqrt{E/\rho}$, and the characteristic impedance is $Z = A\rho c$.

The normal forces at x_A and x_B are related to the measured strains through

$$N_A(t) = AE\varepsilon_A(t) \qquad N_B(t) = AE\varepsilon_B(t) \tag{8}$$

respectively. The particle velocity $V_A(t)$ at X_A is related to these quantities by

$$v_A(t) = v_A(t_P) + \frac{1}{Z}[-N_A(t) - N_A(t_P) + 2N_B(t - T_{BA})] \tag{9}$$

where $t_P = t - 2T_{BA}$ and $T_{BA} = (X_B - X_A)/c$. From $N_A(t)$ and $v_A(t)$ the corresponding quantities at the cross-section x_E at the end of the rod can be determined from the relations

$$\begin{aligned} N_E(t) &= \frac{1}{2}[N_A(t + T_{EA}) + N_A(t - T_{EA})] \\ &\quad + \frac{Z}{2}[v_A(t + T_{EA}) - v_A(t - T_{EA})] \\ v_E(t) &= \frac{1}{2}[v_A(t + T_{EA}) + v_A(t - T_{EA})] \\ &\quad + \frac{1}{2Z}[N_A(t + T_{EA}) - N_A(t - T_{EA})] \end{aligned} \tag{10}$$

where $T_{EA} = (x_E - x_A)/c$. The load-point displacement $u(t)$ and the applied force $F(t)$ can be expressed as

$$u(t) = \int_0^t v_E(\tau)d\tau \tag{11}$$

$$F(t) = -N_E(t) \tag{12}$$

Determination of Specimen Stiffness

If only the first mode of vibration is present, and in the absence of damping, the specimen can be modeled as a one-degree-of-freedom system with stiffness k and natural frequency ω. For such a system the theoretical response $u_{th}(t)$ to an applied force $F(t)$ is

$$u_{th}(t) = \frac{\omega}{k}\int_0^t F(\tau)\sin[\omega(t, \tau)]d\tau \tag{13}$$

In our case the force $F(t)$ and the displacement $u(t)$ were known, and k and ω were found by an iterative minimization procedure which minimized the error $\xi(k, \omega)$ defined by

$$\xi(k, \omega) = \int_0^T (u_{th}(t) - u(t))^2 dt \tag{14}$$

where $T = t_i$ is the time of initiation of crack growth. This method has been developed by Popper and Osizmás[13] and is a special version of the generalized secant method.

The method to determine the stiffness of the specimen is especially interesting when the Young's modulus of the tested material is rate dependent, as it is for PMMA. The stiffness is determined during the actual fracture toughness test, that is, with the correct rate of loading.

Detection of the Initiation of Crack Growth

The initiation of crack growth reduces the stiffness of the specimen, and therefore the force applied to the specimen decreases drastically. There will be a time interval between the initiation of crack growth and the decrease of the measured force due to the wave travel time. If the force is evaluated directly on the surface of the specimen, however, this interval will be a minimum.

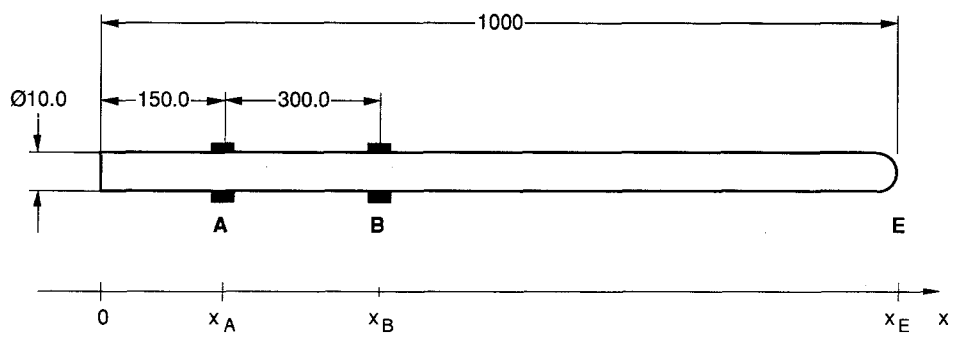

Fig. 2—Modified Hopkinson pressure bar

With strain gages bonded near the notch tip, we have verified that the drastic decrease of the applied force corresponds to the initiation of crack growth. This has been done for specimens of glass as well as of PMMA.

Experimental Method

Experimental Setup

Experimental tests were made with the setup shown in Fig. 3. The Hopkinson bar was impacted by a cylindrical projectile driven by an air gun. A damper was placed between the projectile and the Hopkinson bar to give a smoother incident pulse and thereby reduce three-dimensional effects. The axial strain was recorded at the cross sections A and B. The load-point displacement and the applied force were determined from the measured strains at A and B, according to the two-point strain method.

The Hopkinson bar was made of a refractory austenitic steel (Thyssen Thermax 4841) with a length of 1000 mm and a diameter of 10 mm. The wave-propagation speed was c = 4840 m/s, the density was ρ = 7818 kg/m^3, and the elastic limit was σ_y = 230 MPa. The bar was supported by low-friction slide bearings so that it was free to move axially during the tests. Two different projectiles were used in the experiments. For the tests on PMMA, a steel projectile with length 300 mm and diameter 10 mm was used. The impact velocity was varied in the range of 1.0 to 1.4 m/s. This corresponds to an amplitude of 100 to 140 μ-strain and a duration of 270 μs for the incident pulse. For the tests on glass, a projectile made of PMMA with length 200 mm and diameter 8 mm was used. The impact velocity was varied in the range of 1.8 to 5.7 m/s. This corresponds to an amplitude of 12 to 40 μ-strain and a duration of 320 μs for the incident pulse.

Semiconductive strain gages with a gage factor of 140 (Kulite AFP-350-090) were used to measure the rather small strain. Two pairs of strain gages, forming a full-bridge to eliminate bending contributions, were bonded to each of the cross sections A and B. The bridges were connected to bridge amplifiers (Measurements Group 2210). The strain signals were recorded with two two-channel digital oscilloscopes (LeCroy 9410) with sampling interval of 1 μs. The recorded strain histories were transferred to a computer (Macintosh II) for evaluation.

Calibration and Test of the Measurement System

The gages were calibrated statically using a known weight. Then the measurement system was tested in two ways, with a free end of the Hopkinson bar.

In the first test we used the measured strain at cross section A together with the zero strain condition at cross section E, the free end, to calculate the force at cross section B according to eqs (8)–(10). The result was compared with the force measured at B and is shown in Fig. 4.

In the second test the displacement at the free end E was calculated from measured strains at A and B, and compared with the displacement measured di-

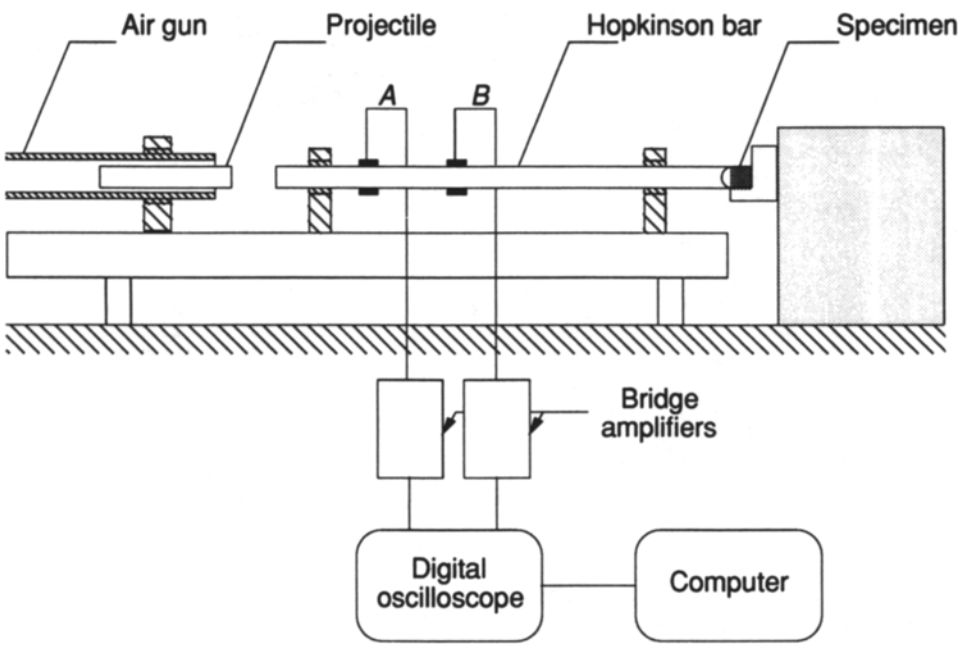

Fig. 3—Experimental setup

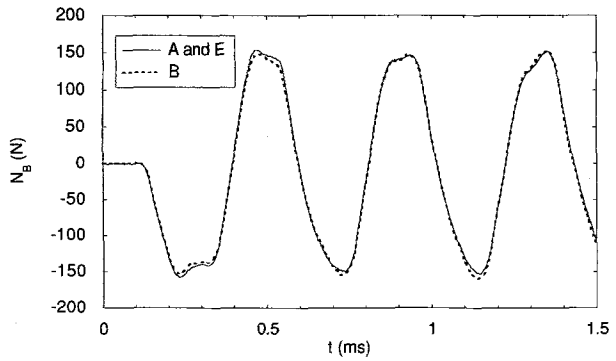

Fig. 4—Normal force N_B at B

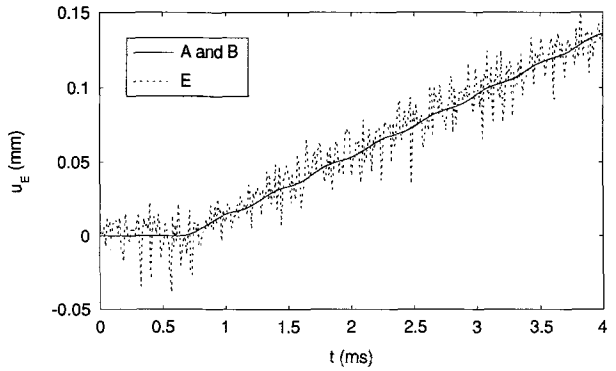

Fig. 5—Displacement U_E at E

rectly by an optical extensometer (Zimmer OHG). The result is shown in Fig. 5.

The good agreements in the two tests indicate that the measured distances, the impedance of the bar, and the wave propagation speed are correct. They also indicate correct sensitivity at the two gage sections.

Results and Discussion

Test of the Method

To test the method we have compared the stress-intensity factor K_I^u, determined from the measured load-point displacement, with the stress-intensity factor K_I^g, derived from strain measurement made on the specimen near the notch. The latter method gives an accurate value of the strain near the notch. However, it cannot be used during high-temperature tests, and it is not well suited for test series with many specimens, as each specimen must be instrumented and calibrated separately.

The strain gage on the specimen was first calibrated statically using the static relation between the applied force and the stress-intensity factor. Since the stress-strain relation is rate dependent for PMMA, we adjusted the calibration factor with respect to the difference in specimen stiffness for static and dynamic loading.

The test was made on a PMMA specimen with a projectile made of PMMA. The impact velocity was low enough not to break the specimen. This gave a long time for comparison. The result is shown in Fig. 6, where the stress-intensity factors determined from the measured load-point displacement, K_I^u, measurement made on the specimen near the notch, K_I^g, and the applied force and the static relation, K_I^s, are compared.

The stress-intensity factor determined from load-point displacement agreed well with the result obtained from strain measurement near the notch tip. In this case the use of the applied force gave an incorrect result. This is due to effects of inertia, as has been noted by several authors, e.g., Kalthoff *et al.*[1]

An evident advantage with the use of measured load-point displacement instead of applied force was the quality of the measurement. The displacement was determined from the time integral of the velocity. Furthermore, the relative error in the evaluated velocity was lower than the relative error in the applied force. This was due to the low stiffness of the specimen. The incident compressive pulse was reflected as a tensile pulse, and the applied force was proportional to the small sum of the strains associated with the incident and reflected waves, whereas the velocity was proportional to the large corresponding difference.

In this test we evaluated the stress-intensity factor from measured strains during 4 ms, which corresponds to a wave travel distance of approximately 20 m in the Hopkinson bar. With the conventional Hopkinson technique, the maximum evaluation time is limited by the length of the bar.

Fracture Toughness Tests

We have made a test series on PMMA specimens to determine the dynamic fracture toughness. The static fracture toughness has been determined for comparison. These tests have been made at ambient temperature.

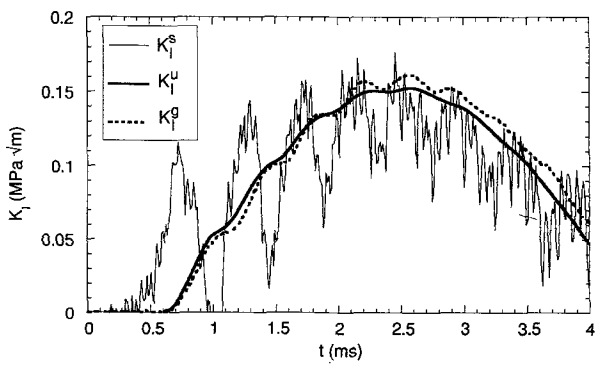

Fig. 6—Stress-intensity factor, K_I

The specimens have been notched by a circular saw with a thickness of 0.2 mm. The geometry of the specimens is shown in Fig. 1, and the dimensions were B = 9.0 mm, W = 10.0 mm, S = 40.0 mm, L = 50.0 mm, and a = 4.0 mm.

The dynamic stress-intensity factor, $K_I^u(t)$, determined from load-point displacement, and the stress intensity factor, $K_I^s(t)$, determined from applied force, in one of the tests on PMMA are shown in Fig. 7. The time to initiation of crack growth was about 600 μs and the period for the first natural frequency of the specimen was 280 μs. The oscillations in the dynamic stress-intensity factor were greater than in the test shown in Fig. 6. This was due to a shorter incident pulse. The frequency of the oscillation corresponds to the wave travel time in the Hopkinson bar. A smoother variation of $K_I(t)$ can be obtained by a longer projectile.

The values of the measured fracture toughness, K_{Id}, are plotted versus the average loading rate, $\dot{K}_I$, in Fig. 8. The results of the tests on PMMA indicate that the dynamic fracture toughness is higher then the static fracture toughness. This tendency has also been reported by Sahraoui.[14] According to his work the static fracture toughness is 1.6 MPa$\sqrt{m}$ and the dynamic fracture toughness is 2.4 MPa$\sqrt{m}$ for $\dot{K}_I$ = 2 MPa$\sqrt{m}$/ms. Our results agree well with these results.

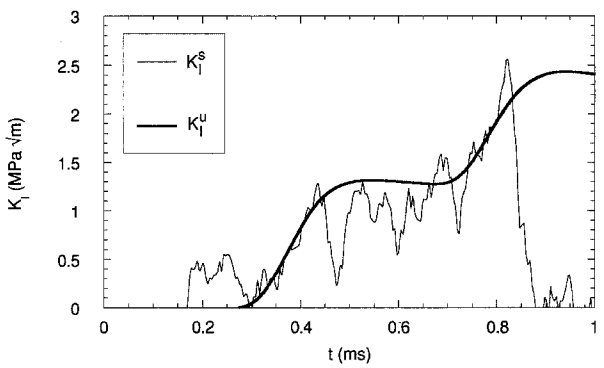

Fig. 7—Fracture toughness test on PMMA

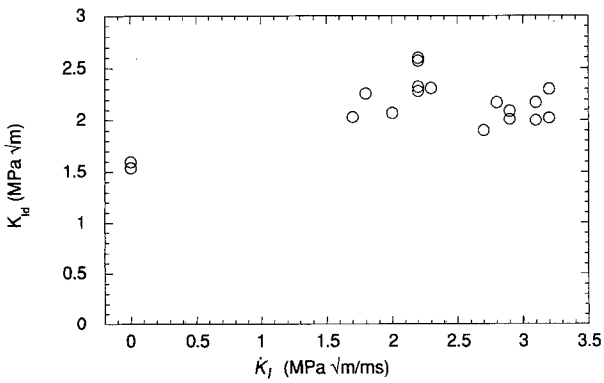

Fig. 8—Measured fracture toughness, K_{Id}, for PMMA

Three series of tests on glass were made. One was made at ambient temperature, one at 200° C, and one at 450° C. Both the dynamic and static fracture toughness have been evaluated in all test series.

The dimensions of the specimens were B = 10.0 mm, W = 10.0 mm, S = 40.0 mm, L = 50.0 mm, and a = 4.0 mm. Two notch widths, w = 0.2 mm and w = 1.0 mm, were used for the tests at ambient temperature, whereas only the notch width w= 0.2 mm was used for the high temperature tests.

The dynamic stress-intensity factor, $K_I^u(t)$, determined from load-point displacement, and the stress-intensity factor, $K_I^s(t)$, determined from applied force, are shown in Fig. 9 for a test at ambient temperature on a specimen with w = 0.2 mm. The time to initiation of crack growth was about 120 μs and the period for the first natural frequency of the specimen was 90 μs.

The values of the measured fracture toughness, K_{Id}, at ambient temperature are plotted versus the average loading rate, $\dot{K}_I$, in Fig. 10. The values of the measured fracture toughness, K_{Id}, at 200° C and 450° C are plotted versus the average loading rate, $\dot{K}_I$, in Fig. 11.

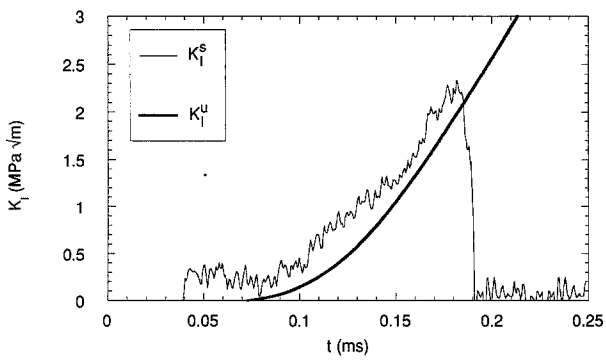

Fig. 9—Fracture toughness test on glass at ambient temperature

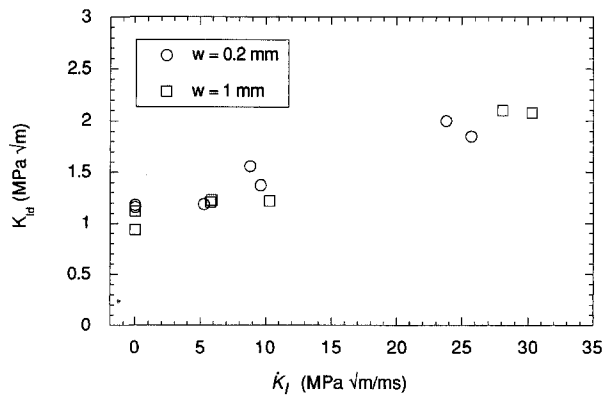

Fig. 10—Measured fracture toughness, K_{Id}, for glass at ambient temperature

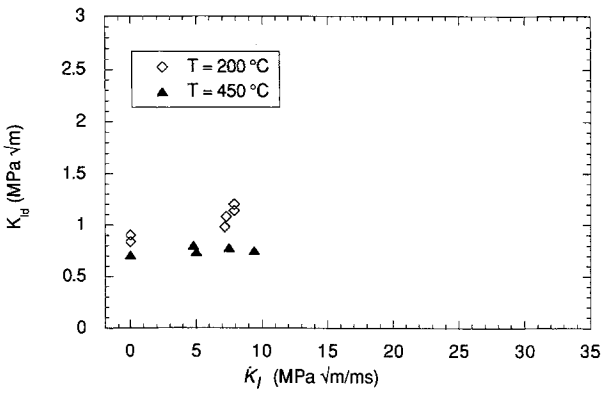

Fig. 11—Measured fracture toughness, K_{Id}, for glass at 200° C and 450° C

The results indicate that the fracture toughness increases with loading rate and decreases with higher temperature.

It should be noted that our results have been obtained from notched specimens, which gives an overestimation of the fracture toughness. The dependence on notch radius of the evaluated fracture toughness has been studied by Kalthoff *et al.*[1] The results in Fig. 10 were obtained from tests on glass specimens with two different notch widths, but the evaluated fracture toughness was approximately the same. This is believed to be explained by the presence of microcracks near the notch tip. Such microcracks were observed on uncracked specimens with a microscope. These microcracks have an irregular shape along the notch tip and this is also believed to explain the variation in the results.

We have shown that the method can be used to determine the dynamic stress-intensity factor even when the effects of inertia are considerable. This makes it possible to determine the fracture toughness at high loading rates.

The fact that all measurements are made at remote cross sections of the bar makes the method well suited for high temperature testing. In our study the maximum temperature was 450° C. We used a bar made of a refractory steel and there was no significant change of material properties. If higher temperatures are used the change of characteristic impedance along the bar can be accounted for by a method developed by Bacon *et al.*[15]

Acknowledgments

The authors wish to thank Professor Bengt Lundberg for his contribution to this work. They are also indebted to the Universities of Lulea and Bordeaux I, the Ministère de la Recherche et de la Technologie, the Région Aquitaine, and Saint-Gobain Recherche for their support.

References

1. *Kalthoff J.F., Winkler S. and Beinert J., "The Influence of Dynamic Effects in Impact Testing," Int. J. Fract.,* **13**, *528–531 (1977).*

2. *Böhme W. and Kalthoff J.F., "On the Quantification of Dynamic Effects in Impact Loading and the Practical Application for K_{Id}-determination," J. de Physique, Colloque C5,* **46** *(8), 213–218 (Aug. 1985).*

3. *Server W.L., "Impact Three-point Bend Testing for Notched and Pre-cracked Specimens," J. Test. and Eval.,* **6**, *29–34 (1978).*

4. *Ramulu M. and Kobayashi A.S., "Dynamic Crack Curving—A Photoelastic Evaluation," Experimental Mechanics,* **23** *(1), 1–9 (1983).*

5. *Kishimoto K., Aoki S. and Sakata M., "Simple Formula for Dynamic Stress Intensity Factor of Pre-cracked. Charpy Specimen," Eng. Fract. Mech.,* **13**, *501–508 (1980).*

6. *Sahraoui S. and Lataillade J.L., "Dynamic Effects During Instrumented Impact Testing," Eng. Fract. Mech.,* **36** *(6), 1013–1019 (1990).*

7. *Nash G.E., "An Analysis of the Forces and Bending Moments Generated During the Notched Beam Impact Test," Int. J. Fract. Mech.,* **5** *(4), 269–286 (1969).*

8. *Ruiz C. and Mines R.A.W., "The Hopkinson Pressure Bar: An Alternative to the Instrumented Pendulum for Charpy Tests," Int. J. Fract. Mech.,* **29**, *101–109 (1985).*

9. *Lundberg B., Carlsson J. and Sundin K.G., "Analysis of Elastic Waves in Non-uniform Rods from Two-point Strain Measurement," J. Sound and Vib.,* **137** *(3), 483–493 (1990).*

10. *Kanninen M.F. and Popelar C.H., Advanced Fracture Mechanics, Oxford University Press (1985).*

11. *Tada H., Paris P.C. and Irwin G.R., The Stress Analysis of Cracks Handbook, Del Research Corp., Hellertown, PA (1973).*

12. *Srawley J.E., "Wide Range Stress Intensity Factor Expressions for ASTM E399 Standard Fracture Toughness Specimens," Int. J. Fract.,* **12**, *475–476 (1976).*

13. *Popper G. and Csizmás F., "Minimization by the Secant Method, an Application to Identification of Frames," Acta Tech. Acad. Sci. Hung.,* **100** *(3–4), 259–267 (1987).*

14. *Sahraoui S., "Effects dynamiques dans les essais de rupture aux grandes vitesses de chargements. Etude de quelques polymères," PhD Thesis No. 876, Univ. of Bordeaux I (1986).*

15. *Bacon C., Carlsson J. and Lataillade, J.L., "Evaluation of Force and Particle Velocity at the Heated End of a Rod Subjected to Impact Loading," J. Physique IV, Colloque C3, 1 (8), 395–402 (Oct. 1991).*